DESIGN AND ANALYSIS OF AIRPLANE WING

T. RamamohanRao, Nithin H.M, C. J. Daniel, Dulla Mayank

Vasavi College of Engineering, Ibrahim Bagh Hyderabad - 31, Telangana State, India.

ABSTRACT

The main work of this project is to design a wing for a commercial air-craft Boeing 747-8 having a wing span of 68.4 meters and a root chord length of 14.36 meters, capable of Trans-sonic cruise (M = 0.85 at an altitude 10.5 km). In this study, the aerofoil for the wing is selected on the basis of 2D flow simulations, the flow is considered as incompressible, steady and turbulent. Then, the wing is modelled with three I section spar, S1223 aerofoil is chosen as the ribs based on 2D flow simulations, Aluminium alloy 7075 is selected as suitable material to reduces the heaviness and to make sure enough toughness. Later the structural analysis is performed and overall deformation, elastic strain and stress are obtained to analysis the behaviour of wing.

Keywords: Aerofoil, angle of attack, spar, Aluminium alloy 7075, C.F.D. analysis, Structural analysis.

I. INTRODUCTION

The designing of airplane wing require knowledge in areas such as Aerodynamics, Machine design, Thermodynamics, Fluid dynamics etc. The main objective of any wing design is that it should be light in weight and withstand various loads. This procedure mainly consists of wing modelling, Structural and C. F. D. analysis. The main objective of this work is to obtain an optimum design for a commercial air-craft Boeing 747-8 wing having a wing span of 68.4 meters and a root chord length of 14.36 meters, capable of Trans-sonic cruise (M = 0.85 at an altitude 10.5 km). Boeing 747-8 is a Fixed-wing and Fixed wings aircrafts are those airplanes which flies using wings that generates lift force with the help of relative windspeed and shape of the wing. The forward thrust force is generated in an airplane by engines present on the wing.

The main function of a wing is to produce sufficient lift for the airplane to fly. The primary aim of wing design is to maximizes lift force and minimizes drag force and pitching moment. An aerofoil usually looks like a positive cambered section that the thicker part is in front of the aerofoil. When air is passed through the aerofoil it will vary the static pressure on the top and bottom surface. The pressure difference between the lower and upper surfaces of wing generates the lift force. Thus, the structural design of the wing is very essential in obtaining the required lift to the aircraft.

Next the design of the wing is accomplished by designing the individual parts of the wing. Before designing the wing, we must first specify the major parts of the wing. The major parts of the wing are ribs, spars, stringers and wing skin.

Ribs are the basic crosspieces that combine with spars and stringers to construct the structure of the wing. The main purpose of the ribs is to maintain the shape of wing, to transmit external applied loads to the wing skin and to reduce column length of stringers and spars. The spar carries flight loads and the weight of the wings while on the ground. Spars are the long beams that provide most of the strength in the aircraft wing and extend from wing root to tip. They provide structural support to the wing while the wing is subjected to lift. Also spars provide support against twisting and upward bending force. Most wing structures have two spars. Modern aircraft wing uses I-section spars.

2. MESHING AND DESIGN METHODOLOGY

2.1 Selection of aerofoil:

Based on the various journals, conference papers, research papers, and other literatures studied, following three aerofoils were selected.

i. Whitcomb aerofoil
ii. NACA 6409 aerofoil
iii. S1223 aerofoil.

The above-mentioned aerofoils are modelled and computational C--type grid domain is meshed in Gambit 2.4.6 as shown in Figure 1 and Figure 2. Then CFD. analysis is performed in ANSYS Fluent 19.1 for the aerofoils travelling at an altitude 10.5 km with Mach number (M) 0.85 and an angle of attack of 0^0. Generally, the aerofoil is located at the mid of a computational domain that goes to a distance of 10 times the chord length, in all directions from the aerofoil’s trailing edge, except at the wake, the aerofoil is located at 15 times the chord length from the trailing edge to accurately produce the wake effect. This is shown in Figure 2.

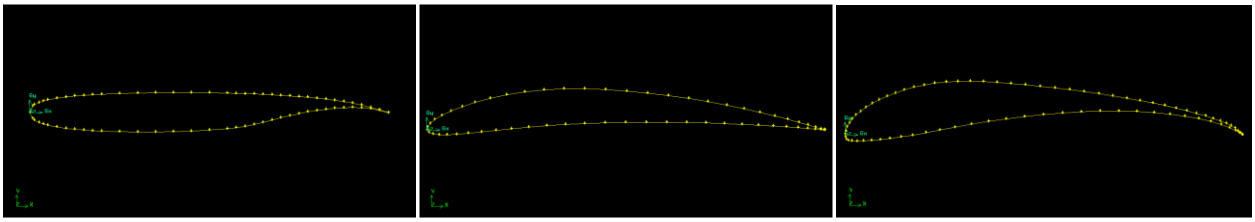

(a) (b) (c)

Figure1: (a) Whitcomb aerofoil model in Gambit 2.4.6
(b) NACA 6409 aerofoil model in Gambit 2.4.6
(c) S1223 aerofoil model in Gambit 2.4.6

Generally, in C.F.D. analysis of an aerofoil the boundary conditions defined are velocity inlet, pressure outlet and aerofoil wall (Stationary with no slip shear condition). For the following CFD analysis viscous-Standard K-ω SST Model is used. Five hundred iteration are performed to minimize the errors in solutions.

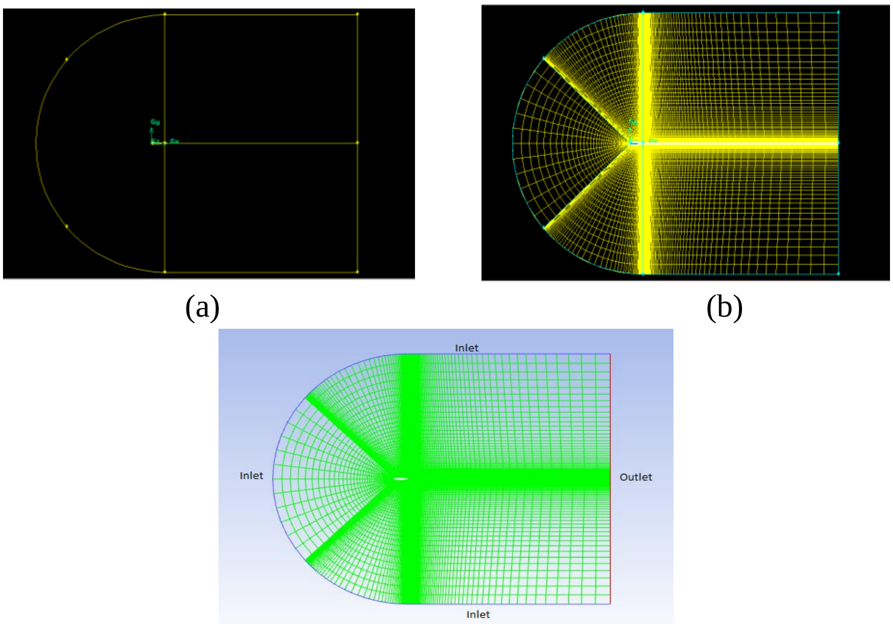

(a) (b)

(c)

Figure 2: a) Geometry and dimensions of Computational domain in Gambit 2.4.6
b) Meshing domain of aerofoil in Gambit 2.4.6
c) Computational domain for aerofoil

The input and boundary conditions used during C.F.D. simulation of the aerofoil are shown in Table 1.

TABLE 1: Fluent parameters

Solver type	Pressure based
Time	Steady
Velocity formulation	Absolute
Model	Viscous-Standard K-ω SST Model
Air Density	0.389 kg/m3
Viscosity	14.4 x 10-5 Ns/m2
Temperature	220 K
Wind speed	254.722 m/s
Pressure	25450 Pascal
Boundary Conditions	Velocity Inlet Pressure Outlet Aerofoil wall: Stationary with no slip shear condition

Method	Scheme: Coupled Gradient (Least Square Cell Based) Turbulent Kinetic energy (Second Order Upwind) Turbulent Kinetic Energy (Second Order Upwind) Turbulent dissipation Rate (Second Order Upwind)

2.2 Wing Modelling:

The dimensions of the wing were obtained from Boeing 747-8 blueprint [Figure 3(a)]. The initial modelling of wing is shown in Figure 2(b) with 3 ribs and the wing skin in SOLIDWORKS 2018. Later the spars were added and the other 9 ribs are added equidistance to each other shown in Fig 4(a)

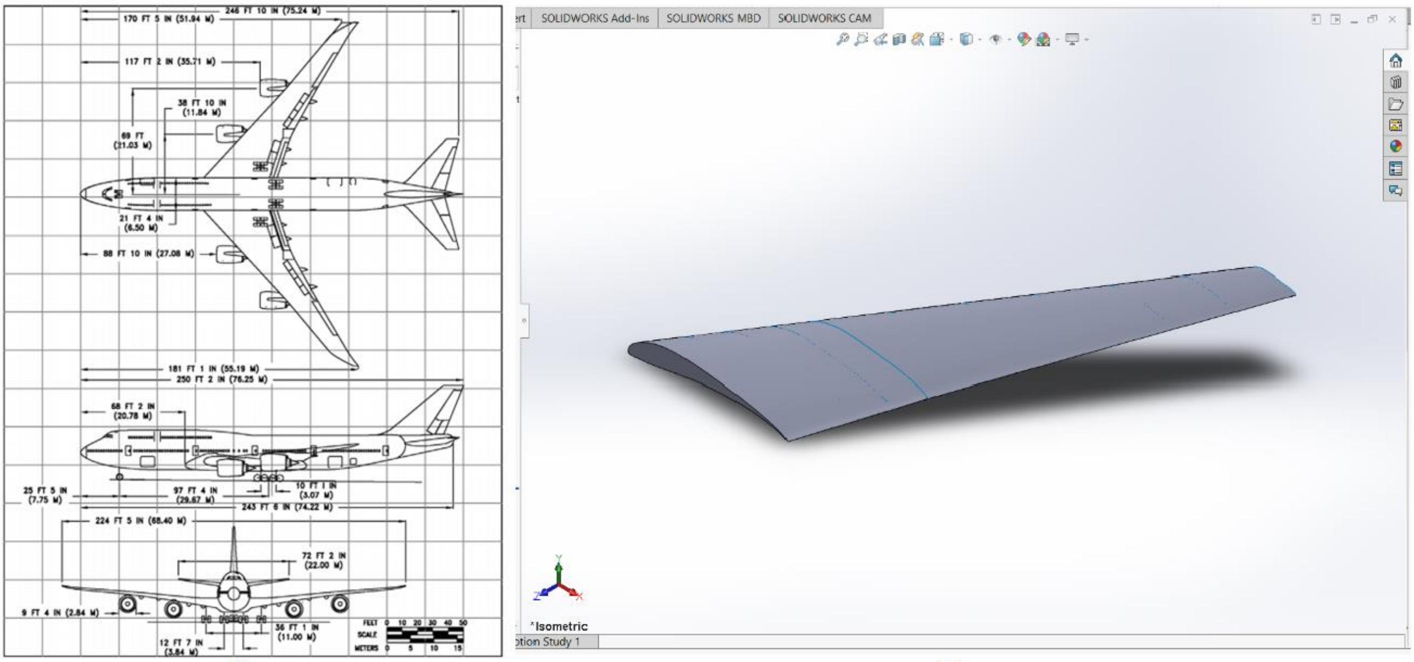

(a) (b)

Figure 3: (a) Boeing 747-8 Blueprint.
(b) Initial model of wing with 3 ribs in SOLIDWORKS 2018

2.3 Materials:

The materials that were tried to use for wing skin, ribs and spars are

i. Structural steel
ii. 316 Stainless steel
iii. Titanium alloy
iv. Ti-6Al-4V
v. Aluminium alloy 7075

Based on the factors such as cost and deflection of wing Aluminium alloy 7075 was finalized for wing skin, ribs and spars. The composition of Aluminium alloy 7075 is shown in Table 2

Table 2: Composition of Aluminium alloy 7075

Material	**Percentage (%)**
Copper	1.2-1.6
Magnesium	2.1-2.5
Zinc	5.6-6.1
Silicon	<0.5
Titanium and other metal	Remaining

2.4 Structural analysis

The structural analysis of wing is performed in ANSYS Workbench 19.1. First, materials considered to be used for the model parts were defined in 'Engineering Data'. Then the wing model was imported and checked in 'Geometry' as shown in Figure 4(a) and Figure 4(b). The properties of model parts are assigned and meshing was performed in 'Model'. The meshed model of wing is shown in Figure 4(c). The forces which were considered for this analysis are shown in Table 3. The root of the wing is fixed. The forces and boundary conditions of wing shown in Figure 4(d) are defined in 'Setup'. The type of solution required was defined in 'Solution' and the solutions were obtained in 'Results'. Based on the results material and model design was modified in 'Engineering Data' and 'Geometry' respectively and the above-mentioned steps were repeated again and again till an optimum design was obtained.

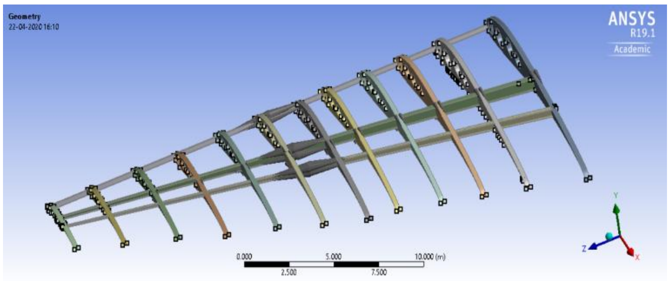

(a)

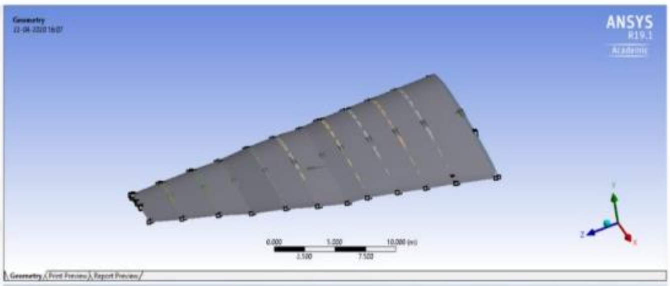

(b)

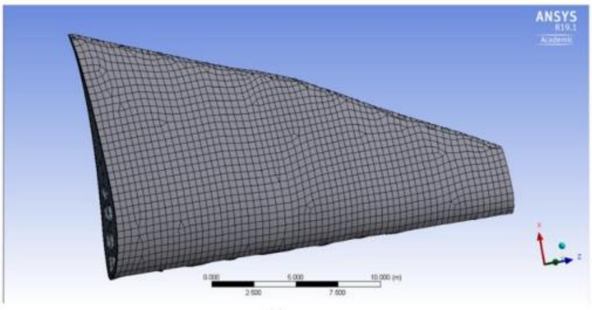

(c)

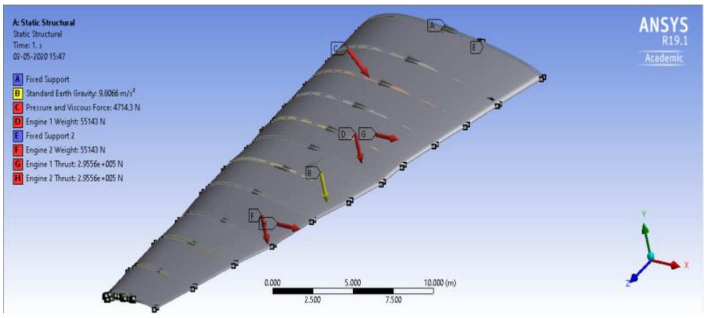

(d)

Figure 4:

a) Internal Geometry of Final Wing Model in ANSYS Workbench 19.1
b) External Geometry of Final Wing Model in ANSYS Workbench 19.1
c) Meshed Model of Final Wing Model in ANSYS Workbench 19.1
d) Forces and Boundary condition in ANSYS Workbench 19.1

Table 3: Forces considered for Structural Analysis

Force	Value	Comments
Pressure Force	3,630N	Obtained from C.F.D. analysis. This value is considered with a Factor of Safety 1.5.
Viscous Force	3,008N	Obtained from C.F.D. analysis. This value is considered with a Factor of Safety 1.5.
Weight of Engine 1 and 2 on wing	55,143N each	Boeing 747-8 airplane consist of two GEnx-2B engines on each wing, which are placed at a distance of 9.92m and 19.11m from the root of the wing.
Thrust Forces due to Engine 1 and 2 on wing	2,95,560N each	Boeing 747-8 airplane consist of two GEnx-2B engines on each wing, which are placed at a distance of 9.92m and 19.11m from the root of the wing
Material Weight of wing	----	The material weight of wing is auto-generated by the software.

3. RESULTS AND DISCUSSION

3.1 C. F. D. analysis Results:

From C. F. D. analysis, the pressure plot, velocity plot, turbulence plot and lift and drag coefficients of Whitcomb, NACA 6409 and S1223 aerofoils were obtained (Figure 5). On comparing the coefficient of lift it was found S1223 aerofoil had the highest lift coefficient among the three aerofoils i.e. 0.97747 [Figure5(a)]. The pressure and viscous force experienced by the aerofoil was found to be 2419.3023N and 2004.7103N respectively.

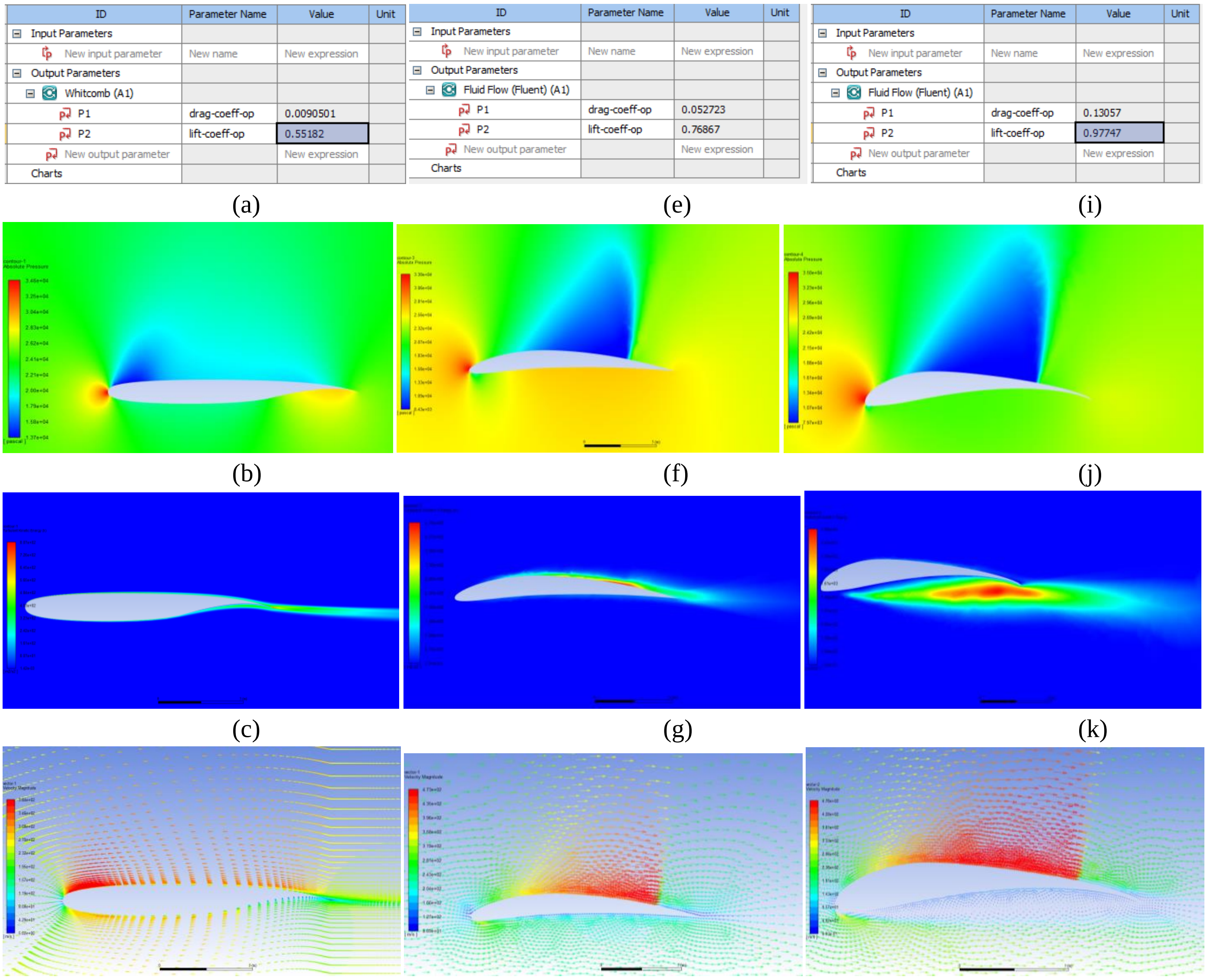

ID	Parameter Name	Value	Unit
Input Parameters			
New input parameter	New name	New expression	
Output Parameters			
Whitcomb (A1)			
P1	drag-coeff-op	0.0090501	
P2	lift-coeff-op	0.55182	
New output parameter		New expression	
Charts			

ID	Parameter Name	Value	Unit
Input Parameters			
New input parameter	New name	New expression	
Output Parameters			
Fluid Flow (Fluent) (A1)			
P1	drag-coeff-op	0.052723	
P2	lift-coeff-op	0.76867	
New output parameter		New expression	
Charts			

ID	Parameter Name	Value	Unit
Input Parameters			
New input parameter	New name	New expression	
Output Parameters			
Fluid Flow (Fluent) (A1)			
P1	drag-coeff-op	0.13057	
P2	lift-coeff-op	0.97747	
New output parameter		New expression	
Charts			

Figure 5:

a) Coefficient of drag and lift value of Whitcomb aerofoil at 0^0 angle of attack.
b) Pressure contours of Whitcomb aerofoil at 0^0 angle of attack.
c) Turbulence Vector contour of Whitcomb aerofoil at 0^0 angle of attack

d) Velocity Vector contour of Whitcomb aerofoil at 0^0 angle of attack
e) Coefficient of drag and lift value of NACA 6409 aerofoil at 0^0 angle of attack
f) Pressure contours of NACA6409 aerofoil at 0^0 angle of attack
g) Turbulence Vector contour of NACA6409 aerofoil at 0^0 angle of attack.
h) Velocity Vector contour of NACA6409 aerofoil at 0^0 angle of attack
i) Coefficient of drag and lift value of S1223 aerofoil at 0^0 angle of attack
j) Pressure contours of S1223 aerofoil at 0^0 angle of attack
k) Turbulence Vector contour of S1223 aerofoil at 0^0 angle of attack
l) Velocity Vector contour of S1223 aerofoil at 0^0 angle of attack

3.2 Structural analysis Results:

A wing is related to a cantilever beam maximum deformation is encountered at the free end and minimum at the fixed end. From Structural analysis, the deformation, stress and strain plot of final wing model is obtained Figure 6. The final internal and external wing design is depicted in Figure 4. Displacement contour of spar is shown in Figure 6(a) and Figure 6(b). The maximum deformation of 0.049524m is found at the free end and at the fixed end there is no deformation. The Table 4 displays how much the maximum wing deflection for number of elements is considered for meshing.

The deformation convergence is obtained up to three decimal points. The uniform Distributed load is considered at the bottom of the wing because of the high pressure for lift has to generate so the force acts on the wing from the bottom. And point load of jet engine weight of 55.14 KN is added at the location of 9.92m and 19.11m from the attachment of the body i.e., from the Chord Root. The Wing is maintained under an earth gravity of 9.8066 m/s^2. The thrust given by the single engine is 295.96KN. Generally, the term stress is used to express the loading in terms of force applied to a certain cross-sectional area of an object. The stress distribution may or may not be uniform, depending on the nature of the loading condition. The stress on the wing skin is shown in Figure 6(f) and 6(g). In case of tapered I-section spar the area on which force is acting is reduced when we move from root to tip so stresses increase as shown in Figure 6(f).

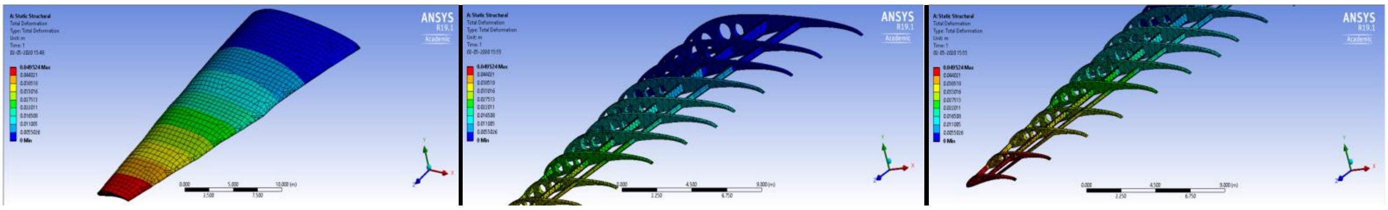

(a) (b) (c)

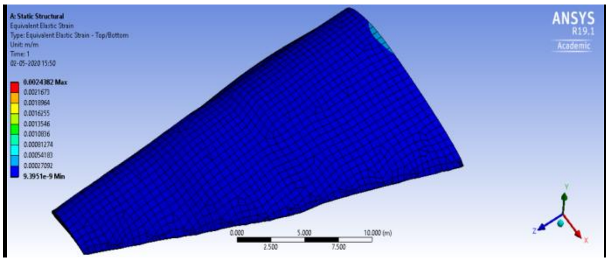

(d)

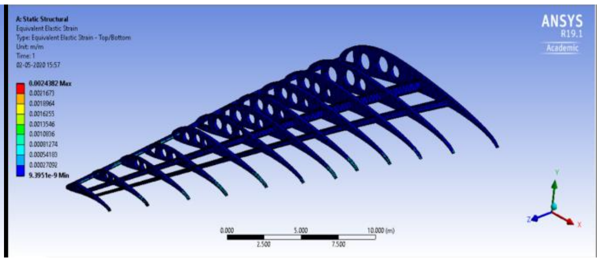

(e)

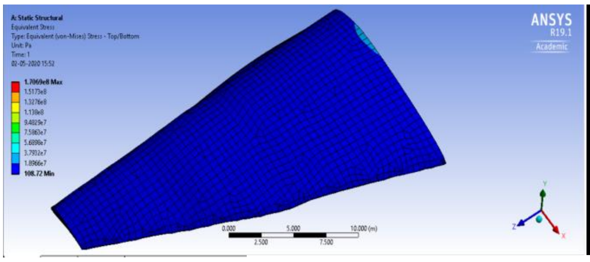

(f)

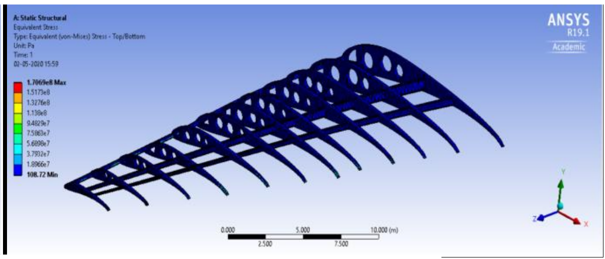

(g)

Figure 6: a) Deformation plot of External wing structure

b) Deformation plot of internal wing structure at root
c) Deformation plot of internal wing structure at tip
d) Strain plot of External wing structure
e) Strain plot of internal wing structure
f) Stress plot of External wing structure
g) Stress plot of internal wing structure

S.NO	NUMBER OF ELEMENTS	DEFORMATION / DEFLECTION (M)
1	9358	0.042983
2	9852	0.042498
3	9894	0.04337
4	10234	0.04428
5	10923	0.044938
6	11116	0.04546
7	11700	0.045819
8	12525	0.04599
9	13132	0.049339
10	13406	0.049359
11	14634	0.049524

Table 4: Convergence

4. CONCLUSIONS

I. The maximum lift coefficient was generated by S1223 among the selected three aerofoils for an angle of attack of 0^0 at an altitude of 10.5km. Based on the C. F. D. analysis results S1223 aerofoil was selected for the ribs of the wing.

II. Based on the Structural results, it was concluded that wing with twelve ribs (S1223 aerofoil shaped) and three tapered I-section spars (two W21x17 and one W21x17)

[Figure 4] with Aluminium alloy 7075 as wing skin, spars and ribs was optimum design for Boeing 747-8 wing.

Acknowledgement:

Sincerely we acknowledge our deep sense of gratitude to all teaching and non-teaching faculties of Vasavi College of Engineering, Ibrahimbagh, Hyderabad, Telangana, India who directly or indirectly guided us and helped us to complete our work.

References:

[1]Stanford BK and Dunning PD. Optimal Topology of Aircraft Rib and Spar Structures under Aeroelastic Loads. Journal of Aircraft. 2015; 52;1298-1311.

[2]Ebrahim H. CFD analysis of the aerodynamic characteristics of biconvex airfoil at compressible and high Mach numbers fow. SN Applied Sciences. 2019:1;1283

[3]Koay KK and Tan WC. Computational Fluid Dynamics study for aerofoil. ISBN: 978-967-0120-04-1; Universiti Malaysia Pahang. 2010: 739-746

[4]Megson TH. Aircraft Structures for engineering students. Butterworth-Heinemann; Elsevier, 2016. Fourth Edition. ISBN-13: 978-0-75066-7395, ISBN-10: 0-750-667397..

[5]Kundo AK. Aircraft Design. Cambridge Aerospace series; United States of America by Cambridge University Press, New York, ISBN-13 978-0-521-88516-4.

[6]El Khchine Y and Smriti M. Boundary layer and mesh refinement effects on aerodynamic performances of horizontal axis wind turbine (HAWT). International Journal of Mechanical Engineering. 2017; 17: 2. ISSN: 2367-8968

[7]Praveenkumar U and Chullai ET. Design & Analysis of Natural Laminar Flow Supercritical Aerofoil for Increasing L/D Ratio Using Gurney Flap. International Journal of Innovative Research in Science, Engineering and Technology (IJIRSET). 2016; 5: 2347-6710.

[8]Mirza MA, Zakuan BM, Aabid A and Khan SA. Modelling and Structural Analysis of Three-Dimensional Wing. International Journal of Engineering and Advanced Technology (IJEAT). 2019; 9: 2249-8958.

[9]Ajith VS, Paramasivam R and Vidhya K. Study of Optimal Design of Spar Beam for the Wing of an Aircraft. International Journal of Engineering Development and Research (IJEDR). 2017; 5: 2321-9939.

[10]Sureka K and Meher RS. Modeling and Structural Analysis on A300 Flight Wing by using ANSYS. International Journal of Mechanical Engineering and Robotics Research. 2015; 4: 123-130.

[11]Von Mises R. The Airplane Wing. Theory Of Flight. Courier Coorporation. 2003 reprinted:112-284.

[12]Atmeh GM, Hasan Z and Darwish F. Design and Stress Analysis of a General Aviation Aircraft Wing. InExcerpt From the Proceeding of the COMSOL Conference 2010 Boston. 2010

[13]Liu D, Xu X, Li Q , Jiang M and Peng X. Numerical Investigation on the Reynolds Number Effects of Supercritical Wing. Fifth International Conference on Intelligent Systems Design and Engineering Applications. 2014; 635-640

[14]www.boeing.com revised edition December 2012 blueprint of 747-8